IOP Conf. Series: Journal of Physics: Conf. Series **1037** (2018) 052014 doi:10.1088/1742-6596/1037/5/052014

Wind turbine aerodynamic measurements using a scanning lidar

C L Kelley[1], T G Herges[1], L A Martinez[2] and T Mikkelsen[3]

[1]Sandia National Laboratories, Wind Energy Technologies, Albuquerque, NM, USA.
[2]National Renewable Energy Laboratory, National Wind Technology Center, Boulder, CO, USA.
[3]Technical University of Denmark, Department of Wind Energy, Roskilde, Denmark.

E-mail: clkell@sandia.gov

Abstract. A method for measuring wake and aerodynamic properties of a wind turbine with reduced error based on simulated lidar measurements is proposed. A scanning lidar measures air velocity scalar projected onto its line of sight. However, line of sight is rarely parallel to the velocities of interest. The line of sight projection correction technique showed reduced axial velocity error for a simple wake model. Next, an analysis based on large-eddy simulations of a 27 m diameter wind turbine was used to more accurately assess the projection correction technique in a turbulent wake. During the simulation, flow behind the turbine is sampled with a nacelle mounted virtual lidar matching the scanning trajectory and sampling frequency of the DTU SpinnerLidar. The axial velocity, axial induction, freestream wind speed, thrust coefficient, and power coefficient are calculated from virtual lidar measurements using two different estimates of the flow: line of sight velocity without correction, and line of sight with projection correction. The flow field is assumed to be constant during one complete scan of the lidar field of view, and the average wind direction is assumed to be equal to the instantaneous wind direction at the lidar measurement location for the projection correction. Despite these assumptions, results indicate that all wake and aerodynamic quantity error is reduced significantly by using the projection correction technique; axial velocity error is reduced on average from 7.4% to 2.8%.

1. Introduction

A scanning lidar, with sufficient spatial and temporal resolution, allows for unique experiments on wind turbines and studies of the complex flow field downstream of a wind turbine in its wake. One such instrument is the SpinnerLidar designed by the Technical University of Denmark [1] and recently deployed in a test campaign at Sandia's Scaled Wind Farm Technology (SWiFT) site [2, 3] on the nacelle of a Vestas V27 wind turbine. The experiment quantified wind turbine wakes [4], the efficacy of wake steering through intentional yaw [5], and the impact of these steered wakes on plant energy capture and unsteady loads. This paper is focused on how to best derive aerodynamic quantities from these scanning lidar measurements. This makes it possible to measure integral aerodynamic performance (for example thrust and power coefficient) without the need for an instrumented blade. There are complicating issues in this analysis: the lidar measurement is the projection of the actual velocity vector into the line of sight (LOS) direction, which prevents the lidar from measuring the true velocity vector, or all orthogonal velocity components, often referred to as the Cylcops problem. An additional complication is

the probe volume averages this velocity projection in space along the laser beam. These issues introduce error to the wake and aerodynamic quantities being derived from a lidar measurement.

The line of sight projection correction technique is first evaluated with a simple wake model in section 2. Next, a more realistic wake simulation of a Vestas V27 wind turbine is used to further test the lidar correction for a realistic, turbulent flow field. The simulation parameters are summarized in section 3. These simulations allowed the exact wake and aerodynamic quantities (no spatial averaging or projection error) to be compared to the virtual lidar measurements, and the associated errors to be quantified. Section 4 focuses on axial velocity, section 5 on measuring freestream wind speed, and section 6 discusses aerodynamic properties such as induction, thrust, and power in the wake as estimated by a virtual scanning lidar.

2. Line of sight projection correction

The velocity measured by a lidar is the actual velocity projected onto the line of sight direction. If α is the angle between these two directions, then from the definition of the vector dot-product it is known that

$$|\mathbf{V}_{LOS}| = |\mathbf{V}| \cos(\alpha). \tag{1}$$

The line of sight projection correction, dividing by the cosine of the subtended angle, α, has been used before for field tests of wind energy research lidars to solve for wind direction offset for aligning a lidar with sonic anemometers [6] and calibration of lidars [7].

If it is assumed the average wind direction is parallel and steady everywhere in the lidar measured flowfield, and the position of the lidar beam is known at every instant of time, then α is known, and the actual wind magnitude can be solved for, $V_{LOSPC} = \frac{V_{LOS}}{\cos(\alpha)}$. This method will be referred to as line of sight projection correction (LOSPC). Due to turbulence, the average wind direction is not equal to the instantaneous velocity direction, but the outcome of this assumption is the focus of this paper.

The average wind direction is known in this paper from the simulations to be parallel with the axis of rotation. If applied to an experiment, the average wind direction would need to be measured separately from the lidar with a wind vane or sonic anemometer for example. The LOSPC method can only be applied after probe volume spatial averaging takes place. So there will always be error that cannot be corrected due to probe volume spatial averaging.

Figure 1a estimates the error for a simple wake model with LOSPC for a nacelle mounted lidar. The velocity field is 1 outside the wake, and $\frac{2}{3}$ inside the wake. Rays emanating from the lidar source had spatial averaging applied and the axial velocity error was found. The maximum error occurs at the edge of the wake where the velocity field changes rapidly and spatial averaging most affects the measurement. For example, measuring the velocity just inside the wake is biased high by the high momentum fluid outside the shear layer of the wake. The velocity error on the black arc with a focal distance of $3D$ is shown in figure 1b. The lidar overestimates the velocity magnitude inside the wake edge (as much as 24%) and underestimates the velocity outside the wake edge (as much as 18%). In addition, it can be seen that a velocity measurement using a lidar near a high gradient has higher error. The LOSPC showed significant improvement in axial velocity error, especially near the periphery of the field of view (FOV). Forsting et al. modeled the error associated with the volumetric averaging of measuring the wake flow field behind a wind turbine [8]. Their results showed similar error, approximately 25–30%.

3. Simulation parameters for virtual lidar testing

A large-eddy simulation of the V27 wind turbine was performed in SOWFA with stable atmospheric conditions by Churchfield [9]. SOWFA implements the actuator line representation of the rotor, which uses a FAST model of the V27 for lift and drag forces. This simulation used a uniform 10 m resolution grid that is 3 km in each direction along the ground, and

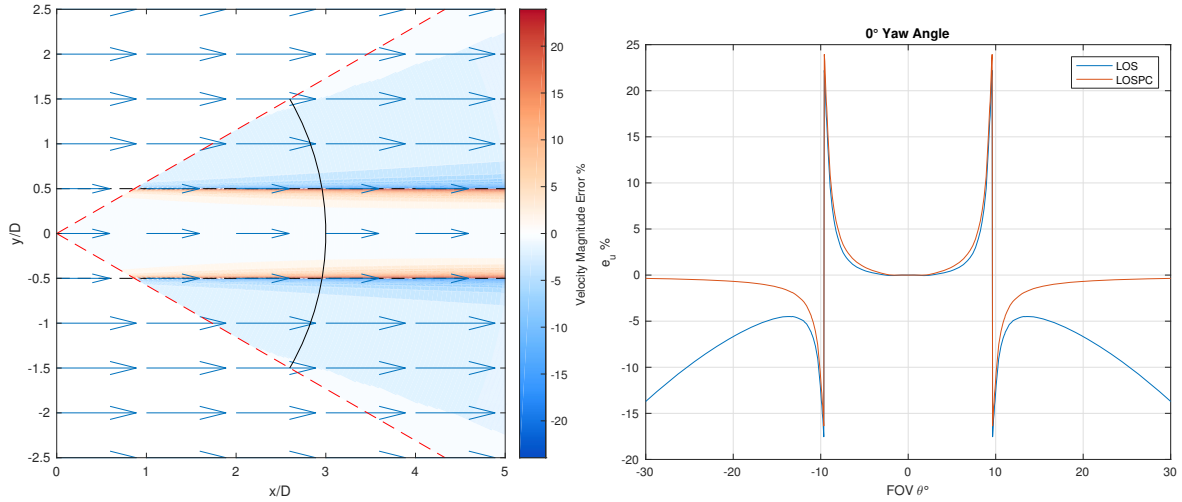

Figure 1. Simple wake model for LOSPC error of axial velocity due to probe volume averaging a) contour b) at a focal length of 3D.

1 km vertically. The time-step was 0.02 s. The hub height average wind speed was 6.5 m/s, the turbulence intensity was 8.5%, and the shear exponent was 0.29. These are representative inflow conditions for the Sandia SWiFT facility in Lubbock Texas [10]. The wind turbine had no average yaw; therefore the wake appears in the center of the field of view for the analyzed conditions. The simulation data analyzed lasted 200 seconds or 100 wake scans.

A virtual scanning lidar was implemented to sample the velocity field with the same operation as the DTU SpinnerLidar. It samples in a rosette pattern of 984 points in 2 seconds with a half-cone angle of 30° and looks downstream from the nacelle into the wake. With a focal distance of 3D (81 m), the volumetric averaging is described by full width at half maximum of 12.1 m with Lorentzian distribution weighting [11].

4. Axial velocity estimation from virtual lidar measurements

The axial velocity was found with a virtual lidar sampling of the SOWFA simulation solution at a focal distance of $3D$ (81 m) downstream of the rotor plane. On this spherical cap surface the exact axial velocity (u_{ex}), the line of sight velocity (u_{LOS}), and the line of sight velocity with projection correction (u_{LOSPC}) were found and can be seen in figure 2 for one lidar scan. u_{LOS} is found by equating axial velocity with the lidar line of sight measurement including spatial averaging. u_{LOSPC} is found by applying the projection correction to u_{LOS}. Axial velocity refers to the velocity component parallel to the wind turbine nacelle.

The wake edge and center are defined by a modified version of the wake tracking algorithm developed by Herges [12] that forces the area of the wake to be twice the area of the rotor disc. The wake edge is found iteratively as the locus of contiguous points of equal LOS velocity such that the enclosed area is equal to $2A_{rotor}$ (originally A_{rotor} for Herges). The wake center is the weighted centroid of LOS velocity within the identified wake region. Actuator disc theory shows that the far-wake area is twice the rotor disc area if static pressure has recovered to freestream static pressure and axial induction is $\frac{1}{3}$. This is a reasonable assumption for wake measurements beyond $3D$ downstream [13] and for rotors with a high power coefficient. The black line and center dot indicate the wake edge and wake center in figure 2.

The differences in the velocity field are subtle, so the error of axial velocity was found as the

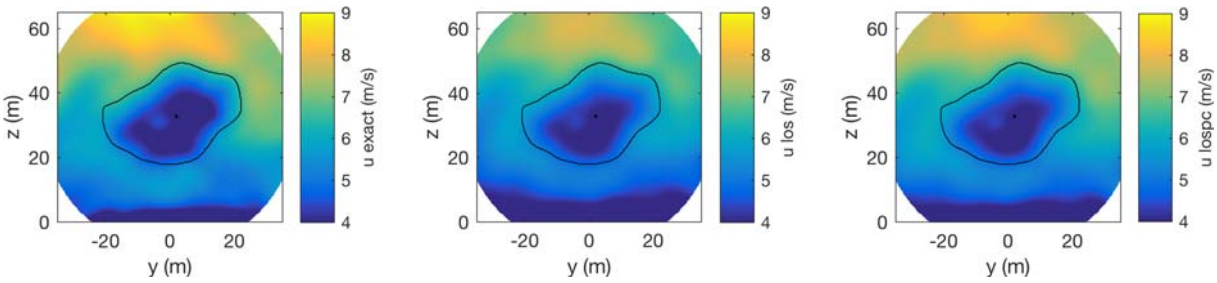

Figure 2. Axial velocity field a) exact, b) line of sight, and c) line of sight projection correction for one scan of the field of view.

difference between the lidar measurement and the exact axial velocity field

$$e_{u_{LOS}} = \frac{u_{LOS} - u_{ex}}{u_{ex}} \tag{2}$$

and

$$e_{u_{LOSPC}} = \frac{u_{LOSPC} - u_{ex}}{u_{ex}}. \tag{3}$$

Figure 3a shows the axial velocity error spatially during one lidar scan (2 seconds). In general, the wake velocity is overpredicted towards the center of the wake, and underpredicted outside the wake in agreement with the simple wake model described earlier. To improve upon the axial velocity measurement by the lidar, the line of sight projection correction technique (LOSPC) was applied and is plotted in figure 3b. Outside the wake, and towards the periphery of the FOV, the error is brought closer to zero, indicated by a greater area of white. The shape of the error need not represent the wake edge.

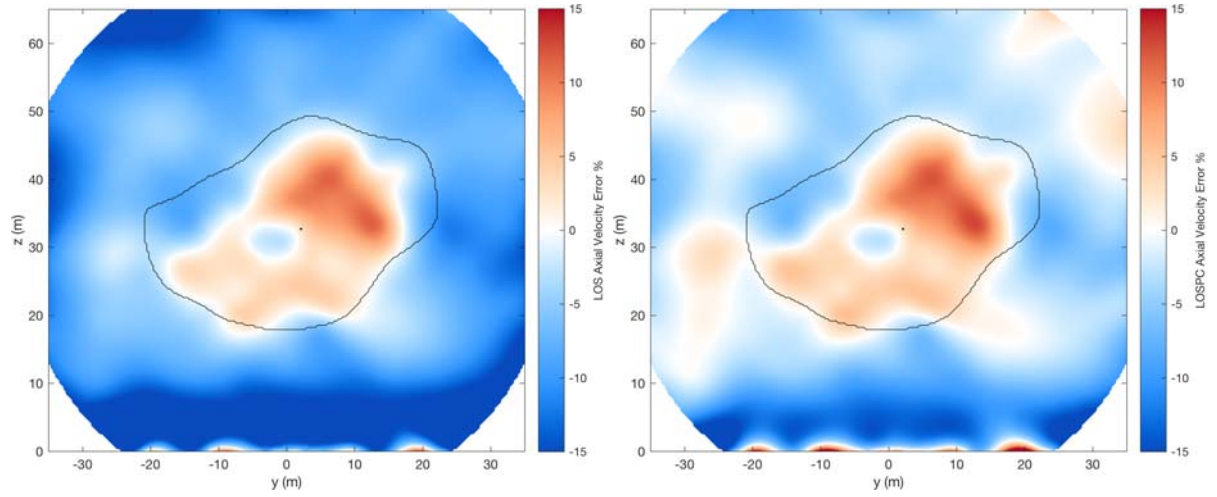

Figure 3. Axial velocity error from a) LOS and b) LOSPC for one scan of the field of view.

A total of 100 FOV scans for a time evolving wake were collected from the simulation. The error associated with the LOS axial velocity and LOSPC axial velocity for the entire field of view and all scans were aggregated into probability density functions. Figure 4a shows that inside the wake, LOSPC improves axial velocity error minimally. Outside the wake, figure 4b shows that the LOSPC is useful in improving the error on average, and reducing the standard

deviation of the error. Over the entire FOV for all 100 lidar scans, LOS axial velocity has an error of -7.4% and the LOSPC axial velocity has an error of -2.8%. The small local maximum of high error at the ground is due to volume averaging in a high shear region.

The remaining 2.8% bias error after LOSPC can be explained by violation of the assumption that average wind direction is equal to an instantaneous velocity direction. Mikkelsen et al. showed that a standard deviation of wind direction of 10° due to turbulence explains an underprediction of axial velocity of 1.5% [14]. This compounded by volumetric averaging across the shear layer of a wake likely explains the 2.8% underprediction after LOSPC.

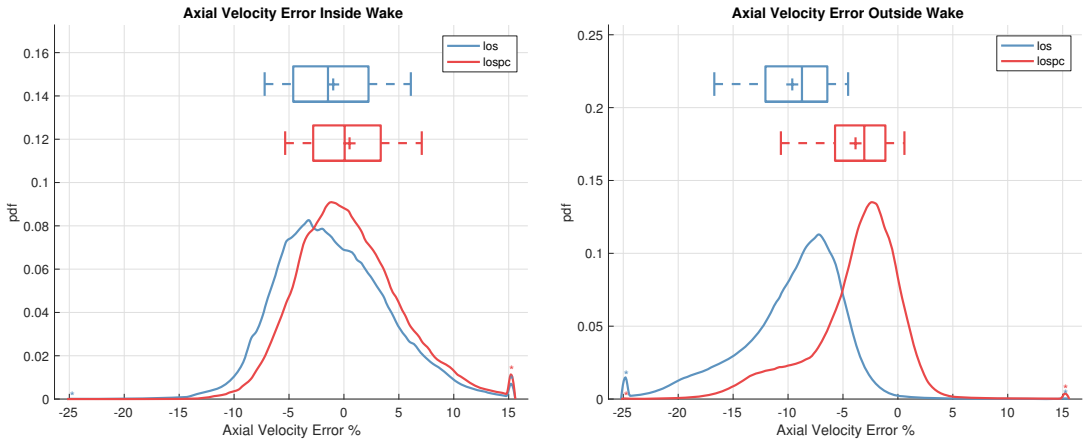

Figure 4. Distribution of axial velocity error at $3D$ for 100 lidar scans a) inside the wake b) outside the wake.

5. Freestream wind speed estimation from virtual lidar measurements

By averaging the velocity field across horizontal slices and by limiting the data points to those outside the wake, the boundary layer profile was measured using the scanning lidar. Figure 5 shows an instantaneous wind speed field with the wake ignored. The horizontal black line corresponds to the V27 hub height, 32.1 m. The projection correction technique reduces the error to give a more accurate prediction of the freestream velocity. Horizontal shear is removed by averaging horizontal lidar slices. Momentum mixing across the wake edge and speedup due to blockage may introduce error in this method of estimating freestream velocity.

The average error of freestream velocity using the LOS measurement was 9.2% below the actual freestream velocity. Using the LOSPC approach the freestream velocity error was brought closer to zero, 3.5% below the exact freestream velocity. Freestream velocity at hub height is a necessary quantity to calculate induction, thrust coefficient, and power coefficient. A meteorological tower could measure hub height wind speed more accurately, however it is not located where the lidar measurement is taking place. Therefore, the freestream velocity measured with the lidar gives an instantaneous value at the lidar measurement plane.

6. Aerodynamic estimation from virtual lidar measurements

The virtual lidar measurements at a focal distance of $3D$ were used estimate aerodynamic rotor quantities from the wake such as axial induction, thrust coefficient, and power coefficient.

6.1. Azimuthal average wake induction

In blade element momentum theory, the axial induction is representative of how much the axial velocity is slowed down by an infinite number of slender blades at the rotor disc, and the axial

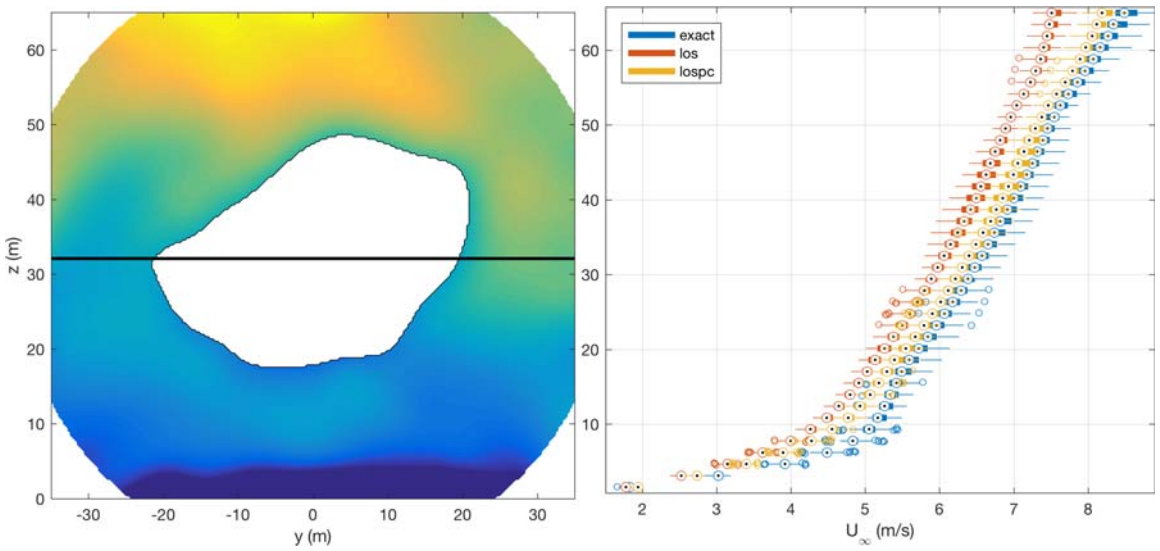

Figure 5. Atmospheric boundary layer a) vertical plane $3D$ downstream and b) freestream velocity from 100 lidar scans.

induction is constant in the azimuthal direction. This theory inspired the following approach whereby the wake may distort and expand in shape from a perfect circle to a more generic shape, as identified by the wake tracking algorithm, and the average induction on each annulus was found.

To find the azimuthal average induction, contours are overlaid on the lidar scan of the wake from the center to the edge to define the distorted annuli seen in figure 6. On each distorted annulus, the average induction was found according to equation 4, where θ is the parameterized angle along the wake arc length.

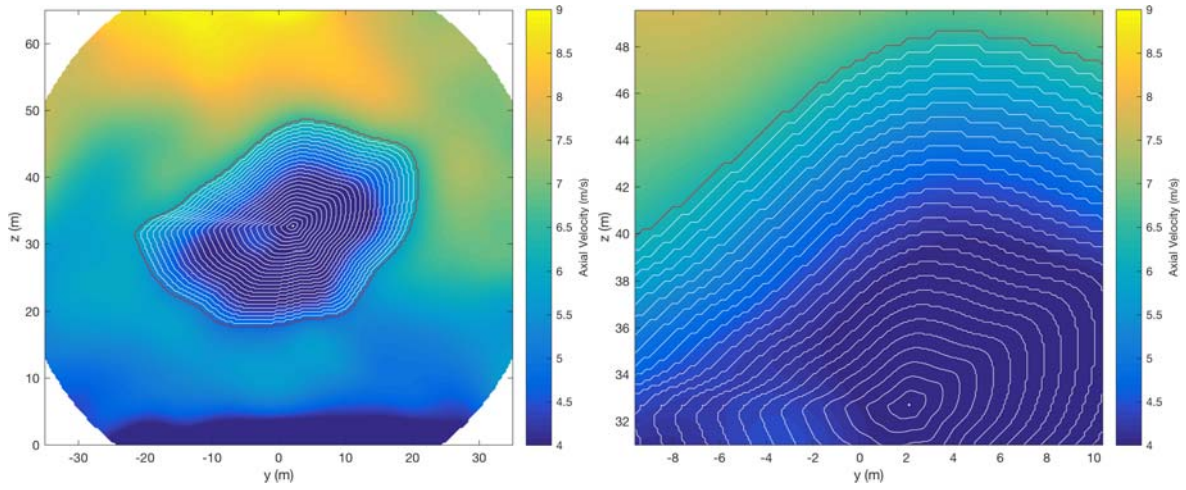

Figure 6. Distorted wake shape annuli and zoomed view.

$$\overline{a} = \frac{1}{2\pi} \int_0^{2\pi} \left(1 - \frac{u_{wake}}{U_\infty}\right) \mathrm{d}\theta \tag{4}$$

Figure 7 shows the results of calculating wake induction, $\overline{a}$, for each distorted annulus, where

$\frac{r}{R}$ is the normalized distance from the wake center ($\frac{r}{R}$=0) to the wake edge ($\frac{r}{R}$=1). The wake shows a half bell curve shaped velocity profile, and the error bars correspond to $\pm\sigma(\overline{a})$ of the 100 lidar scans. Consistent with figure 3, the LOS and LOSPC lidar measurement introduces spatial averaging error inside the wake that overpredicts axial velocity, therefore the axial induction is seen here to be underpredicted compared to the exact.

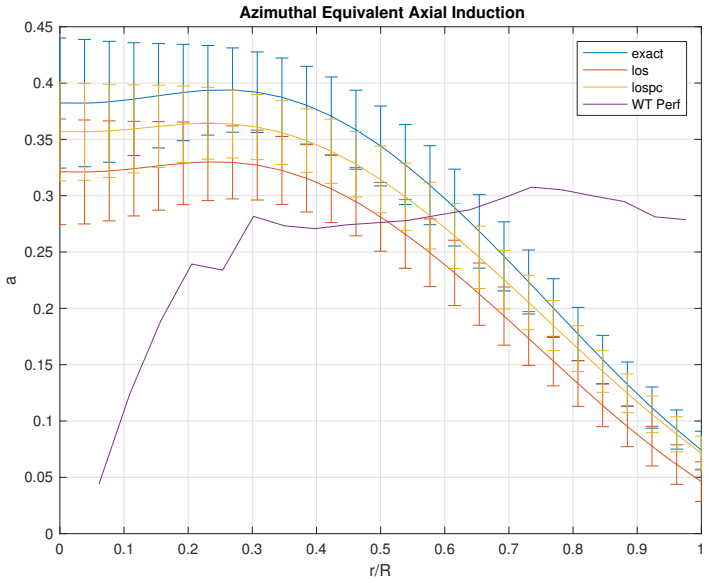

Figure 7. Azimuthal averaged wake induction for 100 lidar scans.

Figure 7 also shows the axial induction at the rotor plane modeled with blade element momentum theory code, WT_Perf. The effect of nacelle drag and streamtube mixing are observed because the radial induction profile in the wake does not match the blade loading at the rotor disc. Therefore one cannot equate mass flow from each distorted wake annulus to the rotor disc annulus to solve for the rotor disc induction. However, if the focal length of the lidar was reduced from $3D$ to closer to the rotor disc, it may be possible to measure the blade load distribution in the wake. For the DTU SpinnerLidar, the minimum focal distance is $1D$ to capture the entire wake in the FOV with current optics.

6.2. Thrust coefficient

The thrust coefficient describes the momentum deficit in the wake. If the deficit is measured in the far-wake, where pressure has recovered, the momentum deficit is also equal to the thrust on the rotor. The thrust force found by integrating the momentum deficit at the actuator disc is half the thrust found by integrating the momentum deficit in the far wake because the static pressure at the rotor disc is not freestream static pressure. A derivation of thrust for a wind turbine wake control volume is presented in Frandsen [13]. The thrust coefficients were found for 100 lidar scans of the simulation at a focal length of $3D$. The freestream velocity was found from a horizontal slice at hub height for each frame. The axial velocity, $u(z, y)$, was taken from the virtual lidar measurements, and the various correction methods were applied. Height above the ground is z meters, and parallel to the ground is y. The x coordinate is the axial flow direction, and it is assumed that the spherical cap is close to a flat plane, and therefore x is constant. The rotor radius of the V27 is turbine $R = 13.5$ m. The area of integration was limited to the wake, and not the entire FOV.

$$C_{T_{wake}} = \frac{2}{\pi R^2} \iint\limits_{wake} \frac{u(z,y)}{U_\infty} \left(1 - \frac{u(z,y)}{U_\infty}\right) \mathrm{d}z\,\mathrm{d}y \tag{5}$$

Figure 8 shows the distribution of thrust coefficients calculated for 100 lidar scans. The LOSPC is beneficial because the mean value of thrust is closer the exact value, and the spread of thrust for the various scans is reduced. LOSPC therefore reduces bias error and random error. The average thrust coefficient error is improved from -15.1% to -4.6%.

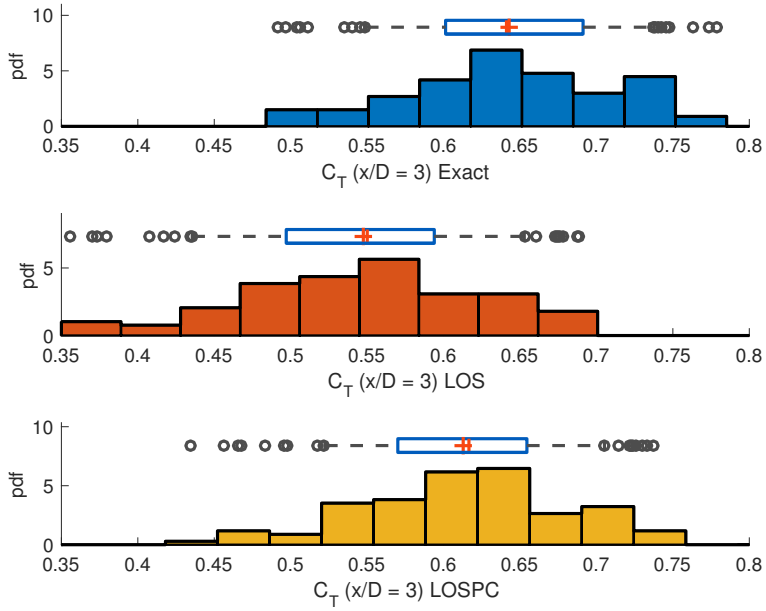

Figure 8. Probability density of thrust coefficient from 100 lidar scans at $f = 3D$.

6.3. Power coefficient

Just as with the thrust coefficient, power coefficient can also be measured from the wake.

$$C_{P_{wake}} = \frac{1}{\pi R^2} \iint\limits_{wake} \frac{u(z,y)}{U_\infty} \left(1 - \frac{u^2(z,y)}{U_\infty^2}\right) \mathrm{d}z\,\mathrm{d}y \tag{6}$$

The power coefficient was found for the same 100 lidar scans of the wake and can be seen in figure 9. Again, the LOSPC brings the calculated power coefficient closer to the exact value and improves error from -13.2% to -3.5%.

7. Conclusions

A simple wake model with a top-hat profile showed that a lidar has the greatest amount of error due to spatial averaging where the velocity field has the largest gradient, in the wake shear layer. The simple wake model motivated further evaluation of the LOSPC technique.

To examine the LOSPC technique in more realistic conditions, a SOWFA simulation with a virtual DTU SpinnerLidar was used to investigate error correction on wake and aerodynamic parameters. All parameters were calculated solely from virtual lidar measurements, knowing the average wind direction, and the lidar position in time. Table 1 summarizes the improvement in error.

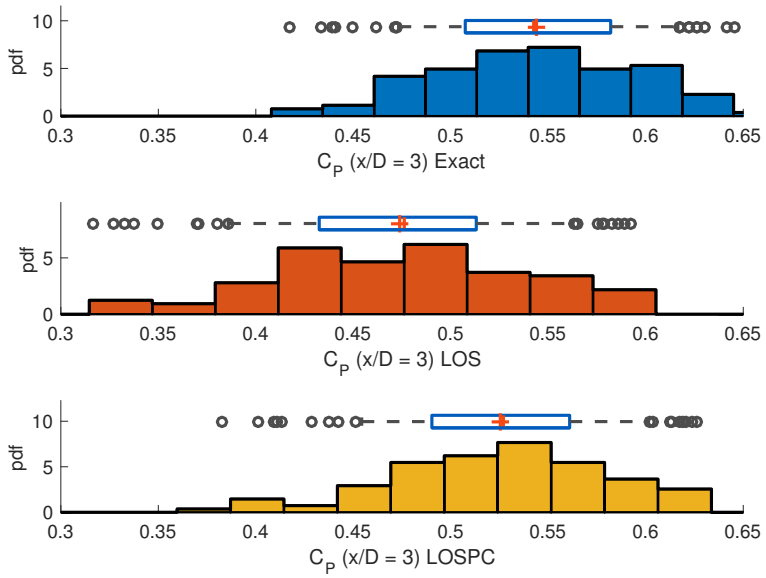

Figure 9. Probability density of power coefficient from 100 lidar scans at $f = 3D$.

Table 1. Summary of Error for Average Values of 100 Lidar Scans.

Method	u (m/s)	u_{error}	$\overline{a}$	$\overline{a}_{error}$	U_∞ (m/s)	$U_{\infty_{error}}$	C_T	$C_{T_{error}}$	C_P	$C_{P_{error}}$
Exact	6.0	—	0.29	—	6.5	—	0.64	—	0.54	—
LOS	5.6	-7.4%	0.24	-18.7%	5.9	-9.2%	0.55	-15.1%	0.47	-13.2%
LOSPC	5.9	-2.8%	0.27	-7.6%	6.2	-3.5%	0.61	-4.6%	0.53	-3.5%

In this table, u is the average axial velocity over the entire field of view, $\overline{a}$ is the average induction for all annuli in the wake, U_∞ is the average wind speed for all heights, C_T and C_P are the average thrust and power coefficients, and all quantities are averaged for 100 lidar scans of the wake. Due to the universal improvement of error, the LOSPC is recommended to be applied for all calculated wake and aerodynamic quantities for each lidar scan of the wake.

The projection corrected axial velocity measurements have a remaining bias error of 2.8% underpredicted for the simulated neutral boundary layer and V27 turbine wake. By scaling the LOS velocity by 1.028 and using the LOSPC correction, the average error is brought to zero:

$$u = \frac{1.028\, u_{LOS}}{\cos(\alpha)}. \tag{7}$$

This correction should be investigated further for different atmospheric turbulence intensities and stabilities. The 1.028 scaling factor seems to be correcting any remaining error due to the instantaneous wind direction not being equal to the average wind direction, in conjunction with the effect of volumetric averaging. Therefore different lidar optics, wakes, and velocity fields may have different scaling factors.

To improve the prediction of wind turbine aerodynamics using the lidar, it may be necessary to improve the wake edge detection algorithm, so one does not assume the wake area is twice to rotor disc area. Additionally, thrust and power coefficients presented here were calculated based on steady, axial flow. If the lidar could be used to measure turbulence in addition to velocity, the thrust and power coefficient calculations could be refined to include momentum due to turbulence [13] by subtraction of unsteady terms.

$$C_{T_{wake}} = \frac{2}{\pi R^2} \iint\limits_{wake} \frac{u(z,y)}{U_\infty} \left(1 - \frac{u(z,y)}{U_\infty}\right) - \frac{2}{\pi R^2} \iint\limits_{wake} TI^2(z,y)\,\mathrm{d}z\,\mathrm{d}y \tag{8}$$

$$C_{P_{wake}} = \frac{1}{\pi R^2} \iint\limits_{wake} \frac{u(z,y)}{U_\infty} \left(1 - \frac{u^2(z,y)}{U_\infty^2}\right) \mathrm{d}z\,\mathrm{d}y - \frac{1}{\pi R^2} \iint\limits_{wake} \frac{5u(z,y)}{U_\infty} TI^2(z,y)\,\mathrm{d}z\,\mathrm{d}y \tag{9}$$

There are a few areas where the current work could be improved and are promising areas of future work. A tool that could be used to improve the lidar measurements would be the DTU linearized flow model LINCOM [1]. This would provide an alternative approach for correcting the LOS lidar measurement to wake and aerodynamic quantities, and its computational cost and accuracy should be compared to the LOSPC technique. A new lidar could be designed with a wider FOV so that the induction closer to the rotor disc could be measured before mixing across the wake width occurs. A wide FOV lidar may be a way of measuring spanwise blade loading close to the rotor plane. Thrust and power coefficients could be refined to include momentum due to turbulence if the lidar could measure turbulence intensity. A wide FOV and short focal length lidar would also require the thrust and power coefficients to be written in spherical coordinates due to the highly curved measurement surface.

8. Acknowledgments

The authors would like to thank Matthew Churchfield for providing SOWFA simulations of the V27 wind turbine. The work described in this paper was supported by funding from the DOE Energy Efficiency and Renewable Energys Wind Energy Atmosphere to Electrons (A2e) Program.

References

[1] Mikkelsen T, Astrup P and van Dooren M F 2016 The lidar cyclops syndrome bypassed: 3d wind field measurements from a turbine mounted lidar in combination with a fast cfd solver *18th Int. Symp. for the Advancement of Boundary-Layer Remote Sensing (Varna, Bulgaria)*
[2] Mikkelsen T K, Herges T, Astrup P, Sjöholm M and Naughton B 2017 Wind field re-construction of 3d wake measurements from a turbine-installed scanning lidar *Int. Conf. on Future Technologies for Wind Energy, WindTech (Boulder, Colorado)*
[3] Naughton B, Schreck S and Wright A 2018 A2e wake steering experiment URL `https://a2e.energy.gov/projects/wake`
[4] Fleming P, Churchfield M, Scholbrock A, Clifton A, Schreck S, Johnson K, Wright A, Gebraad P, Annoni J, Naughton B, Berg J, Herges T, White J, Mikkelsen T, Sjöholm M and Angelou N 2016 *J. Phys.: Conf. Series* **753** 052003
[5] Gebraad P, Thomas J J, Ning A, Fleming P and Dykes K 2017 *Wind Energy* **20** 97–107
[6] Schmidt M, Trujillo J J and Khn M 2016 *J. Phys.: Conf. Series* **749** 012005
[7] Borraccino A, Courtney M and Wagner R 2016 *Remote Sensing* **8** 907
[8] Forsting A, Troldborg N and Borraccino A 2017 *J. Phys.: Conf. Series* **854** 012014
[9] Churchfield M, Wang Q, Scholbrock A, Herges T, Mikkelsen T and Sjöholm M 2016 *J. Phys.: Conf. Series* **753** 032009
[10] Kelley C L and Ennis B L 2016 *SWiFT site atmospheric characterization* SAND 2016-0216 (Sandia National Laboratories)
[11] Herges T G, Maniaci D C, Naughton B T, Mikkelsen T and Sjöholm M 2017 *J. Phys.: Conf. Series* **854** 012021
[12] Herges T G, Maniaci D C and Naughton B 2018 Uncertainty quantification framework for wind turbine wake measurements with a scanning lidar *2018 Wind Energy Symposium (Kissimmee, Florida)* 0511
[13] Frandsen S T 2007 *Turbulence and turbulence-generated structural loading in wind turbine clusters* Ph.D. thesis Risø-R-1188(EN)
[14] Mikkelsen T, Angelou N, Hansen K, Sjöholm M, Harris M, Slinger C, Hadley P, Scullion R, Ellis G and Vives G 2013 *Wind Energy* **16** 625–43